Supplementary Information

An ionic liquid-based delivery system of small interfering RNA targeting Bcl-2 for melanoma therapy

Yuyuan Xing[a,b], Yanhui Hu[a,b], Hongyan Wang[a,b], Yanyan Diao[a,b,d,*], Hua Yue[a,b,c,*]

[a]Beijing Key Laboratory of Ionic Liquids Clean Process, CAS Key Laboratory of Green Process and Engineering, State Key Laboratory of Biochemical Engineering, Institute of Process Engineering, Chinese Academy of Sciences, Beijing 100190, P. R. China.

[b]College of Chemical and Engineering, University of Chinese Academy of Sciences, Beijing 100049, P. R. China.

[c]Key Laboratory of Biopharmaceutical Preparation and Delivery, Chinese Academy of Sciences, Beijing 100190, P. R. China.

[d]School of Chemical & Environmental Engineering, China University of Mining and Technology (Beijing), Beijing 100083, P. R. China.

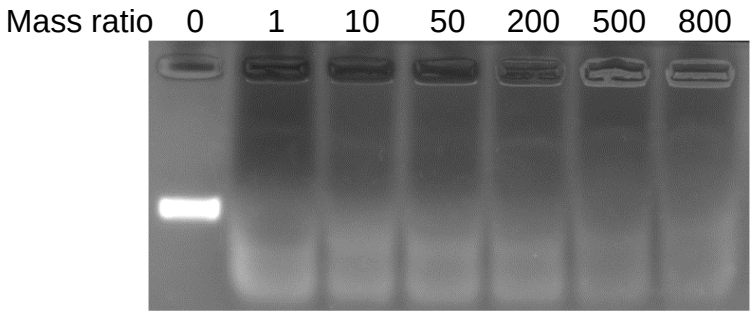

Supplementary Fig. 1 Agarose gel electrophoresis retardation assessment of C6-siBcl-2 using formulations of 0, 1, 10, 50, 200, 500, and 800 mass ratios (C6: siBcl-2, w/w).

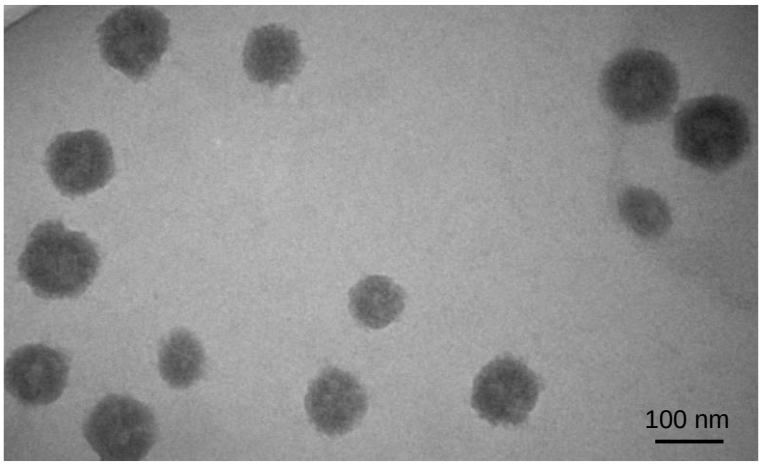

Supplementary Fig. 2 TEM images of C6-siBcl-2.

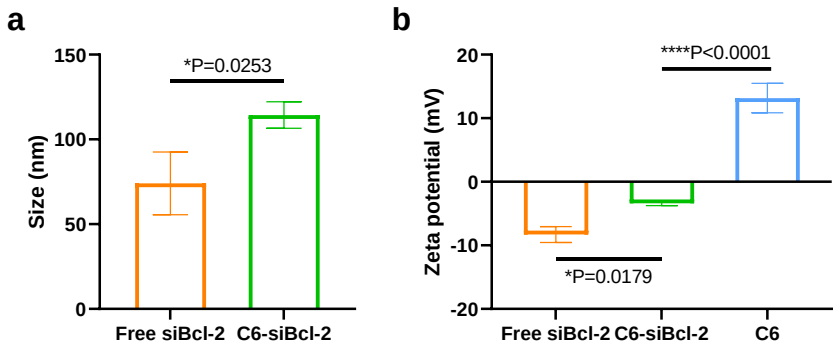

Supplementary Fig. 3 Characterization of C6-siBcl-2. (a and b) The particle diameter (a) and zeta potential (b) of indicated formulations. Data in (a and b) represent the mean ± SD (n = 3). Statistical analysis was performed by Student's *t* test (a) or one-way ANOVA (b).

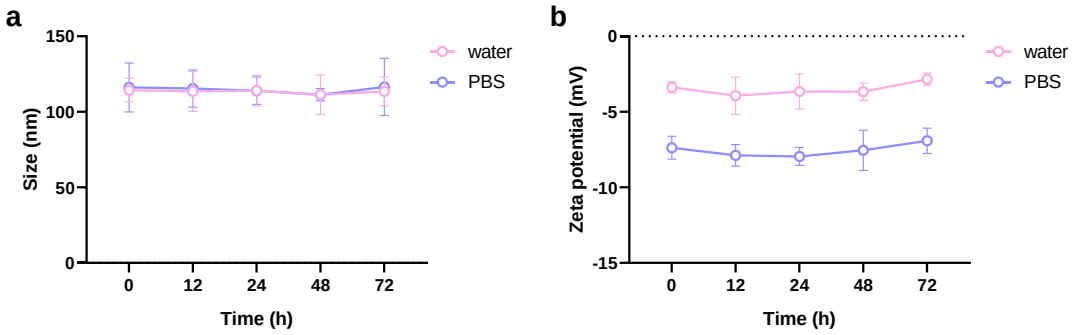

Supplementary Fig. 4 The stability of C6-siBcl-2. (a and b) The particle diameter (a) and zeta potential (b) of the delivery system in water and PBS for different time periods. Data in (a and b) represent the mean ± SD (n = 3).

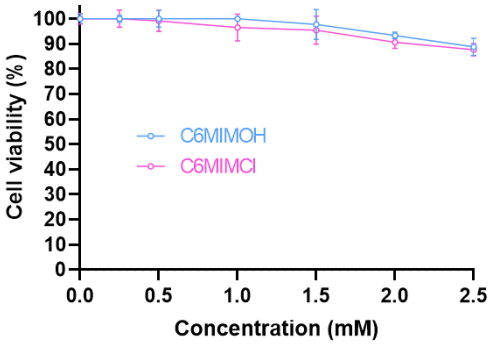

Supplementary Fig. 5 The cytotoxicity of IL carriers before and after ion exchange at different concentrations determined by the CCK-8 assay. Data represent the mean ± SD (n = 3).

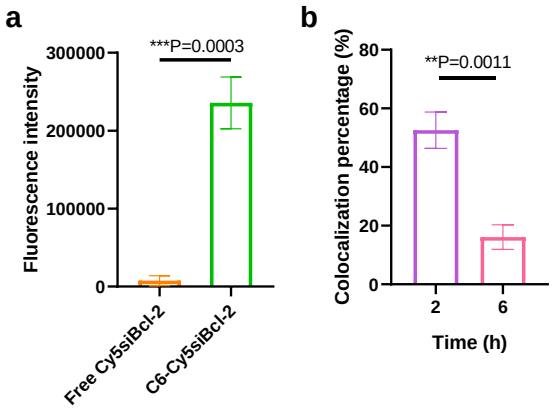

Supplementary Fig. 6 Cell uptake and lysosome escape of delivery system. (a) Fluorescence intensity of Cy5siBcl-2 in free Cy5siBcl-2 and C6-Cy5siBcl-2 groups for Fig. 2. (b) Colocalization analysis of lysosomes (LysoTracker, green) and C6-Cy5siBcl-2 (red) fluorescence signals in B16F10 cells treated with C6-Cy5siBcl-2 for 2 h and 6 h in Fig. 3. Data in (a and b) represent the mean ± SD (n = 3). Statistical analysis was performed by Student's *t* test (a and b).

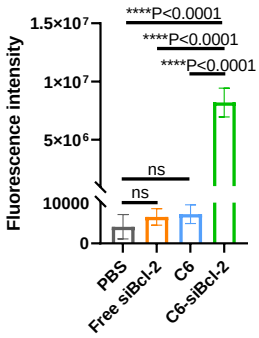

Supplementary Fig. 7 Quantitative analysis of ROS production in B16F10 cells after incubation with PBS, free siBcl-2, C6, or C6-siBcl-2 for 6 h in Fig. 4a. Data represent the mean ± SD (n = 3). Statistical analysis was performed by one-way ANOVA.

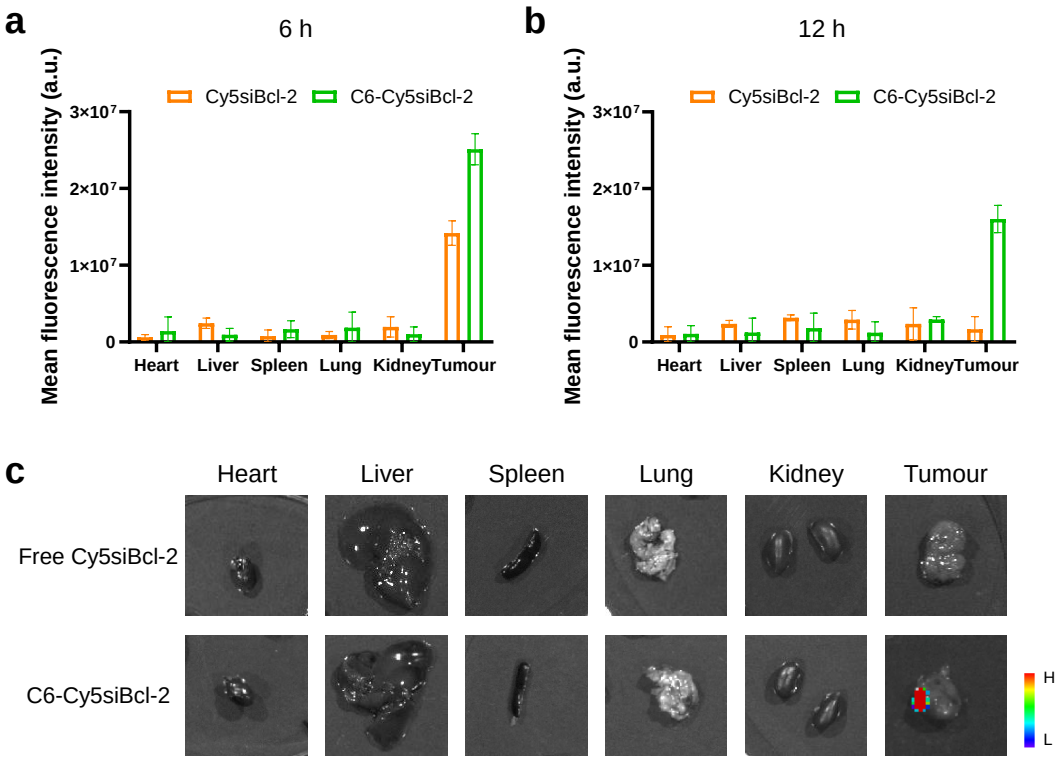

Supplementary Fig. 8 Biodistribution assessment of delivery system on melanoma-bearing mice. (a and b) Quantitative analysis of the siBcl-2 distribution signals after 6 h (a) and 12 h (b) of injection. (c) Representative fluorescence images of the excised organs after 12 h injection of free Cy5siBcl-2 and C6-Cy5siBcl-2. Data in (a and b) represent the mean ± SD (n = 3).

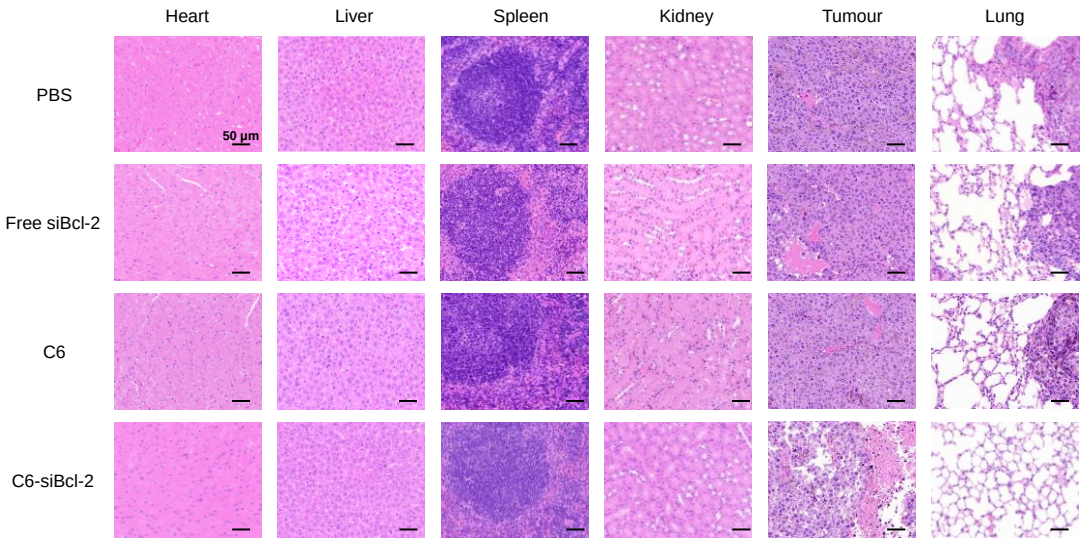

Supplementary Fig. 9 Representative H&E images of major organs and tumours of melanoma-bearing mice treatment with PBS, free siBcl-2, C6, or C6-siBcl-2.

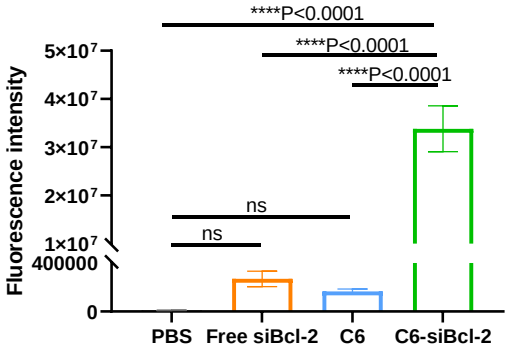

Supplementary Fig. 10 Quantitative analysis of TUNEL immunofluorescence staining in tumour tissues from mice with different treatments for Fig. 7e. Data represent the mean ± SD (n = 3). Statistical analysis was performed by one-way ANOVA.